5

Soft Computing Techniques in Modelling the Influence of pH and Temperature on Dopamine Biosensor

Vania Rangelova[1], Diana Tsankova[1] and Nina Dimcheva[2]
1Technical University – Sofia, branch Plovdiv
2University of Plovdiv
4000 Plovdiv
Bulgaria

1. Introduction

Biosensors represent very promising analytical tools that are capable of providing a continuous, fast and sensitive quantitative analysis in a straightforward and cost-effective way. According to the definition of IUPAC (International Union of Pure and Applied Chemistry) the biosensing analytical devices combine a biological element for molecular recognition with a signal-processing device (transducer). The transducer, which normally ensures the high sensitivity of the sensor, can be thermal, optical, magnetic field, piezo-electrical or electrochemical. On the other hand, the selectivity of detection is assured by the biological recognition element that might consists of either a bioligand (DNA, RNA, antibodies etc.) or a biocatalyst, such as some redox proteins, individual enzymes and enzymatic systems (cell membranes, whole microorganisms, tissues) (Castillo et al., 2004; Scheller et al. 2001). Electrochemical biosensors show two main advantages over the other types of biosensors: i) they are susceptible to miniaturization, and ii) the electrical response – current or potential, could be easily processed using not expensive and compact instrumentation.

Among the electrochemical biosensors, enzyme-based amperometric biosensors represents the most used group, which functions on the basis of monitoring the current variation at an polarised electrode, induced by the reaction/interaction of the biorecognition element with the analyte of interest. Then, amperometric enzyme-based biosensors on their part, can be classified into three categories (Castillo et al., 2004; Scheller et al., 2001), in accordance with the mode of action:

- *first generation biosensors*: the signal is generated upon the electrochemical reaction of an active reagent (monitoring the decrease of the current) or product (monitoring the increase of the current) that are involved in the biochemical transformation of the target compound- the enzyme substrate (Dimcheva et al., 2002 ; Dodevska et al., 2006; Horozova et al., 2009).
- *second generation biosensors*: the architecture of these biosensors includes a freely diffusing redox mediator (small molecular weight compounds, able to effectively shuttle electrons between the electrode surface and the enzyme active site) and in this

Source: Intelligent and Biosensors, Book edited by: Vernon S. Somerset,
ISBN 978-953-7619-58-9, pp. 386, January 2010, INTECH, Croatia, downloaded from SCIYO.COM

mode the concentration of the target analyte, that participate at the biochemical reaction, is proportional to the response resulted from the mediator oxidation/reduction at the electrode (Stoica et al., 2009).

- *third generation biosensors*: the biocomponent is capable of directly (mediatorsless) exchanging electrons between the active site of the enzyme and the transducer and as a result, the concentration of analyte is directly proportional to the redox current generated at the polarised electrode. The advantages of third generation biosensors are represented by the simplicity of construction, the exclusion of additional supportive substances (e.g. mediator), the increase of specificity for target analyte, the removal of interferences due to usually low polarization potential at the working electrode, etc. (Christensson et al., 2004; Stoica et al., 2005). Nevertheless, only limited number of enzymes (mostly heme – or copper - containing oxidoreductases) has been proven to work for the third generation biosensors and their common feature is that a metal-containing cofactor that functions either as a catalytic cofactor and/or as an intra-molecular electron transfer cofactor is embedded in the protein shell.

Despite the second and especially third generation biosensors ensure an exceptional selectivity of the analysis, first generation biosensors are the most widely spread, mainly because of the simplicity of their construction. A typical first generation biosensor can be easily constructed by assembling the biological recognition element onto a conventional electrode, which can be either an oxygen-sensitive probe to assay the consumption of oxygen, or a hydrogen peroxide – sensitive electrode to monitor the concentration of H_2O_2, produced upon the enzymatic conversion of the analyte. Assaying the biological oxygen demand (BOD) seems to be the most universal method for biosensing, since oxygen is the reagent consumed during biochemical transformations catalysed not only by individual oxidative enzymes or enzymatic systems, but also by whole aerobic microorganisms.

Modelling the processes taking place at the interfaces of the first generation amperometric biosensors as well as identifying the factors possessing strong impact on their response will facilitate to a great extent the optimisation of biosensors fabrication, which in turn will considerably shorten the period between R&D stage and their mass–market acceptance. The catalytic activity of the biological recognition element is known to depend strongly on pH and temperature, and therefore these factors are expected to affect the biosensor response as well. Similarly to the chemical reactions, the rate of enzyme-catalyzed reactions rises exponentially with increasing temperature, however this dependence passes through a maximum because at temperatures around 50 deg an irreversible thermal denaturation of the enzymes starts. The dependence of the biosensor response on pH represents a bell-shaped curve that reaches its maximum around the pH optimum of the bio-component. The peak might be broad or narrow, depending on the composition of the medium and temperature. Under the optimal conditions (pH and temperature) the biosensor response is stable and the sensitivity is high and hence, this environment shall be preferred for the measurements.

The modern intelligent devices typically possess the ability to compensate the influences of different kind such as temperature and pH as the later are among the most important factors for an optimal biosensor performance. Modelling the output current versus pH and temperature would provide the opportunity to improve their accuracy and usage while doing measurements under variable conditions.

In the present work a plant tissue biosensor for dopamine assay is considered as the model biosensor, based on a plant tissue immobilized onto an oxygen Clark probe (Rangelova et

al., 2003). Such a biosensing system will be of high interest for the biomedical analysis because the dopamine levels in urine and blood plasma are indicative for diseases like ganglioneuroma, schizophrenia, manic-depressive psychosis, stress, and burn-out syndrome. The traditional analysis is made mainly by radioimmunoassay or chromatography, which are time and labour-consuming techniques, requiring tedious sample pre-treatment and costly equipment. Alternatively, an amperometric dopamine biosensor would provide a fast and straightforward assay of the analyte. Depending on the diffusion limitations the response time of such an amperometric biosensor can range from several seconds to 2-3 minutes.

The purpose of the present work is to model the influence of pH and temperature- separately and simultaneously, on the dopamine biosensor response by means of soft computing. The problem to solve is to find a way of increasing the accuracy (and the rapidity) of the modelling process, under a condition of insufficient experimental data. To this end, the following soft computing techniques were compared in MATLAB environment: (1) *Cerebellar Model Articulation Controller* (CMAC) neural network, (2) *neural network with backpropagation learning algorithm* (NNBP), (3) *fuzzy logic* (FL), and (4) *adaptive-network-based fuzzy inference system* (ANFIS). The relative errors over a few new experimental samples were calculated for validation of the proposed models.

2. The biosensor

2.1 Biosensor construction, the mechanism of enzyme action, experimental setup, measurement procedure, and factors affecting the biosensor performance

a) Biosensor preparation.

The detection principle of dopamine biosensing consists in measuring the oxygen consumption upon the oxidation of dopamine, catalysed by the enzyme polyphenol oxidase (PPO). The first-generation biosensor studied here, was constructed from a conventional oxygen probe (Clark type gold electrode, purity 99.95%, 1 mm diameter) used as transducer and a polyphenol oxidase (PPO) - containing membrane, fixed at the tip of the electrode. A thin banana (*musa acuminata*) slice was used as the source of PPO enzyme. The banana tissue was first homogenised, then immobilised onto a dederone mesh (thickness 70 μm), the mesh was placed over an oxygen-permeable Teflon membrane (10 μm thick) which was further assembled on the forehead of the oxygen electrode. To protect the biological material from leakage, the dederone mesh was covered by a 25 μm thick dialysis membrane and the so obtained triple-layer membrane was fixed with an O – ring onto the forehead of the working electrode.

b) Mechanism of enzyme action

The enzyme polyphenol oxidase (PPO) the physiological function of which is to convert phenolic compounds into *o*-quinones in the presence of molecular oxygen, consists of four subunits containing one atom of copper per subunit (Palmer, 1963), with a relative molecular weight of the tetramer of about 128 000 Daltons. It possesses two binding sites for aromatic compounds including phenolic substrates (Climent, 2001) and a distinct binding site for oxygen. The enzyme reaches its optimum activity at pH 7 when using it specific substrate dopamine – a phenolyc type neurotransmitter. The oxidation of dopamine with molecular oxygen, catalysed by the enzyme PPO is schematically represented by the following reaction (1):

$$\text{Dopamine} + 1/2\ O_2 \xrightarrow{\text{PPO}} \text{Dopamine-o-quinone} + H_2O \quad (1)$$

Or the corresponding general scheme of a bi-substrate enzyme –catalysed reaction:

$$So + C \xrightarrow{E} P \quad (2)$$

where So stands for the first substrate – dopamine, the dissolved oxygen gas (the co-substrate) is denoted with C, with E – the enzyme PPO; with P – the products: dopamine – o – quinine and the molecule of water released upon dopamine oxidation.

c) Experimental setup and apparatus.

The experimental setup is schematically depicted at Fig.1. (Rangelova et al., 2002). All the measurements were performed in a conventional dual-electrode electrochemical setup with the working bio-electrode and a reference Ag/AgCl electrode. Prior to use the biosensor was conditioned by dipping in a phosphate buffer (pH = 7) for one hour. Then the prepared biosensor was immersed in a single-compartment electrochemical cell (working volume 15 ml, filled with phosphate buffer) and polarised at a constant potential of - 800 ± 80 mV/ vs. Ag/AgCl. During the experiments the solution was permanently stirred at 600 rpm (*rpm-rotations per minute* stirring rate, with a magnetic stirrer). Transient currents were allowed to decay to a steady-state value within 2 - 3 min until a constant background current (the response in the buffer solution without substrate) of 104 nA ± 7.5 nA was established. The output current was measured by means of a microampermeter (Φ 195 accuracy ±1.5%, Russia, measuring range 50 nA - 100 μA). For monitoring the transient state a Y - t recorder (ENDIM 622.01, Germany) was used. The pH of the buffer solutions was adjusted with a

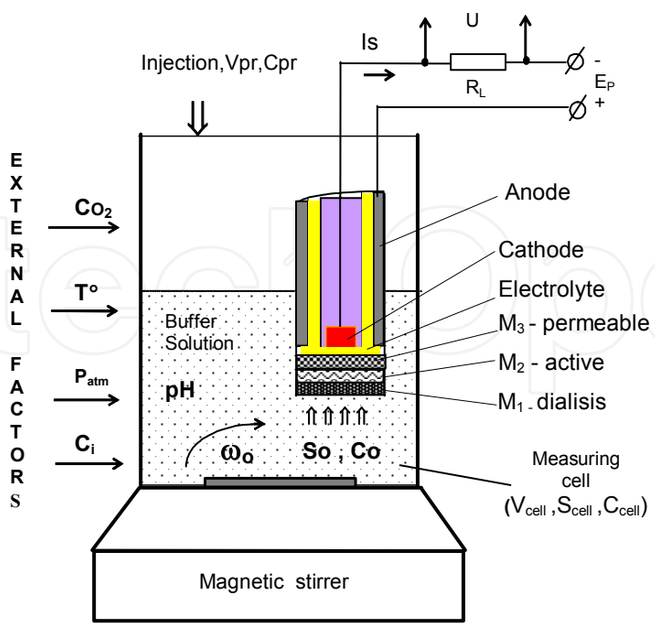

Fig. 1. Schematic representation of the dual–electrode experimental setup

pH-meter Piccolo (Hanna Instr., accuracy ± 0.1), while the temperature was monitored with a mercury thermometer (accuracy ± 0.05°C).
On Fig.1. the three membranes are indicated as follows: M_1 - dialysis, M_2 - the banana tissue-containing membrane and M_3 - the gas-permeable membrane. In the electrochemical cell the working electrode was negatively polarised and therefore functioned as the cathode, while the reference electrode was the anode. The potential difference between the electrodes was generated by applying an external voltage E_P. When the current Is passed through the loading resistance R_L an Ohmic drop U was generated.

d) Measurement procedure

In order to determine any unknown concentration of substrate in the cell ($S_{cell} = S_o$) a calibration graph was built by using the method of subsequent additions. For this purpose, the background current was first established at the chosen pH and temperature, then an aliquot of the substrate stock solution with a volume V_{pr} and concentration C_{pr} was added to the buffer in the cell (volume V_{cell}) and the current was allowed to decay to a steady-state value. Then new aliquots were injected in the cell and the corresponding biosensor responses were registered until the saturation of the enzyme layer with substrate was reached, i.e. until the electrode response stopped changing when a new injection was added. Upon injecting the substrate the transient current was registered with Y-t recorder until the steady state was reached and the readings of microampermeter were taken as electrode response. Usually, 12 additions with volume of 100 μl each, were made and the calibration graph was obtained by plotting the electrode response versus the substrate concentration at which it was registered. Single dopamine injection assures a final concentration of substrate in the cell of S_o=0.142 mM.
In order to provide the enzyme-catalysed reaction with a continuous flow of oxygen, which is the second substrate of PPO, the buffer solution was permanently stirred with a stirring rate ωo, ensuring also much faster mass-transfer of the substrate towards the enzyme layer (the membrane M_2). In this layer the measured substrate So is converted to the product P, a part of the dissolved oxygen is consumed during the dopamine enzymatic oxidation, while the rest of the oxygen passes through the gas-permeable membrane and is further depolarised on the cathode, resulting in an output current I_s. The measurements were performed in a steady-state regime.

e) The influencing factors

The main factors supposed to affect to a great extent the output current of the dopamine biosensor, are schematically depicted at Fig.2. (Rangelova et al., 2002). With block 1) is denoted the dissolution of the oxygen Co_2 from the gas phase to the liquid phase Co. With block 2) is denoted the dilution of the sample concentration Ssm to the measured one So. With block 3) is denoted the conversion of the gas components C_G into the corresponding concentrations in the liquid phase Ci. In the active membrane from the membrane group 4) reaction catalyzed by the enzyme (E) takes place. With Pi is denoted the lateral product from the conversion of substrate S into the product P. They change the acidity of the medium to the value pH_R. In the active membrane, usually the optimal pH and temperature T are maintained. In the active membrane normally the optimal pH is given and for these reason it is changed with ΔpH. Because the system is co-substrate sensitive, through the membrane M_3 the residual concentration of oxygen Cx and only a part of obstructive substances $Ci^{(2)}$ is passing. The rest reagents with concentration $Ci^{(1)}$, product P and substrate S are returned

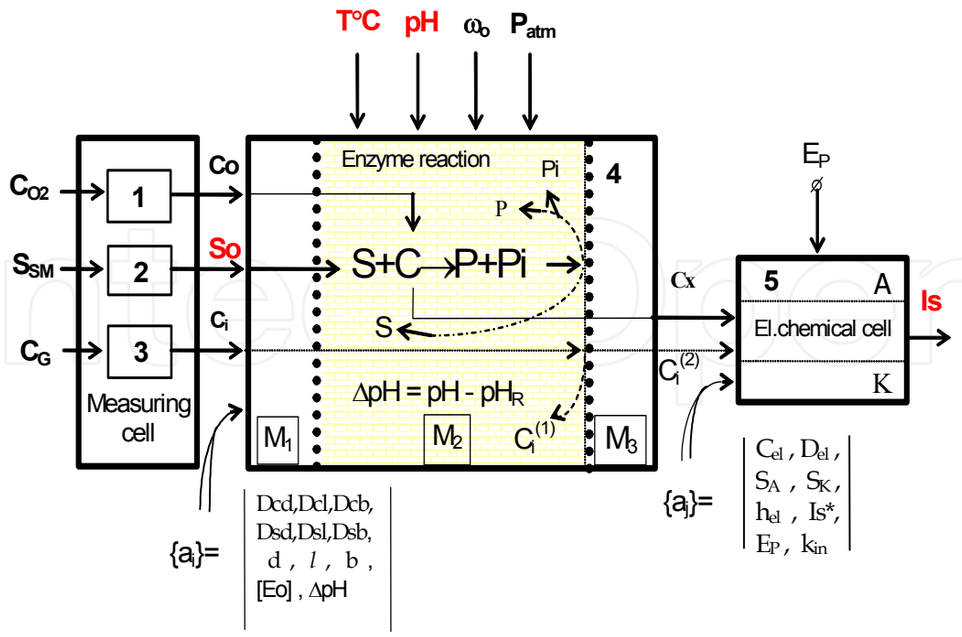

Fig. 2. Scheme of the factors influencing the biosensor responce.

to the active membrane. The electrochemical cell 5) is supplied by an external polarising voltage Ep. The output steady-state current is Is. **The main external factors possessing strong impact over the biosensor performance are: temperature t °C, pH, stirring rate ω_o and atmospheric pressure P_{atm}. They have significant effect over the processes into the measuring cell. For the practical measurements all these parameters are chosen very carefully and the measurements are done for some definite working conditions (depending on the task).** The constructive parameters can be divided into two groups. The *first one* $\{a_i\}$, includes all diffusions coefficients Dij, the thickness of membranes b, l, d, variation of ΔpH and concentration of enzyme [Eo]. The *second group* $\{a_j\}$ includes the parameters of the electrochemical cell: concentration of electrolyte Cel and the corresponding diffusion coefficients Del, the thickness of the electrolyte layer h_{el}, anode and cathode surface area- S_A and S_K, the initial value of the current I*, the value of the polarising voltage Ep and the rate constant of the electrochemical reaction Kin.

From the metrological point of view, the measurements with a biosensor can be presented with the model

$$y = F(x, \xi_1, \ldots\ldots \xi_m, T, a_1 \ldots\ldots a_n, \Delta F)\,, \tag{3}$$

where: x – is the measured value (concentration of substrate So);

$\xi_1, \ldots\ldots \xi_m$ - influencing factors (Co_2 , C_G ,T, pH, ωo, P_{atm});

$a_1 \ldots\ldots a_n$ - constructive parameters ($\{a_i\}$, includes all diffusions coefficients Dij, the thickness of membranes b, l, d, variation of ΔpH, concentration of enzyme [Eo] and $\{a_j\}$ include the parameters of the electrochemical cell : concentration of electrolyte Cel and corresponding diffusion coefficients Del, the thickness of the electrolyte layer h_{el}, anode area S_A and cathode area S_K, the initial value of current Is*, the value of the polarising voltage Ep and the rate of the electrochemical reaction Kin.);

ΔF - error of the model.

For the given biosensor all constructive parameters are chosen after careful selection, depending on the task and usage, but the influencing factors depend on the circumstances and they may change during the measurement. Temperature and pH are the most important influencing factors. They have strong impact not only on the very enzymatic reactions (Ziyan & Pekyardimci, 2004; Shizuko et al., 2005; Burkert et al., 2006) but also on the diffusion parameters (Puida et al, 2009) and the oxygen concentration (Falck , 1997) and therefore the output current will be greatly dependent on them. Moreover, the temperature and pH significantly affect the biosensor response, causing *non-linearity* (maximum in our case) in the curve of the output current.

Thermostatic conditions can be achieved by either controlling the sample solution temperature or by regulating the temperature of the electrode itself so that the membrane and diffusion layers are at a constant temperature throughout an experiment (Falck , 1997). pH can be controlled too. But when the biosensor is used *in-situ* or *in-vivo* (in our case for measurement of neurotransmiter dopamine) the temperature and pH affect strongly the output reading. The body temperature may be higher or lower than the temperature at which the sensor is calibrated and the same is for the pH (depending on the person's acid-base status, the pH of urine may range from 4.5 to 8) thereby it can be invalidating the calibration curve (usually it has been done for constant pH and constant temperature). If thermostatic conditions are not feasible, temperature effects must be compensated. The most popular method is hardware method. Using a miniature thermistor probe, the temperature of the sensing system is measured simultaneously with the current of the biosensor and a normalised signal is calculated which does not depend on temperature (Skladal 1995, Patent Appl. No. 60/859,586, 2006). But those methods can not compensate the full process of measurement. First, pH can not be compensated during the in vivo measurement. Second, the measured current is very small – within the nA- range, where the drift of electronic devices will affect the precision of the whole system. If the biosensor is used for the biomedical purposes, where the accuracy of the device is of key importance, it is necessary to be sure that measured values are real and precise.

The soft computing methods propose a new type of modelling the influence factors over measurement quantity and that way the calibration surfaces for the certain range of them can be received. Those methods are intelligent and adaptive. Their advantages become more obvious when the data are complex.

2.2 Calibration graphs

The experimental data used in the work were derived under the following conditions: Calibration graphs were carried out in steady state regime, using the method of subsequent additions. Every addition was with volume 0.1 ml and corresponding to 0.142 mM dopamine concentration. Measurements were stopped when the saturation zone of the output current Is was reached, because the system became uninformative. *Five* calibration graphs were obtained for five different temperatures (15 24 26 35 and 50°C) at a constant pH=7 and 12 steps of substrate additions (Fig.3a). *Seven* calibration graphs were built up for seven different pH-values (4 4.8 5 5.4 5.8 7 7.5 and 8) at a constant temperature T=24°C and with the same steps of substrate additions (Fig.3b). Because the output current is a dropping function of substrate concentration it was centred to the zero of the scale. The vertical section of Fig.3a and Fig.3b for the given substrate concentration So=0.142 mM is shown in Fig.3c and Fig.3d, respectively.

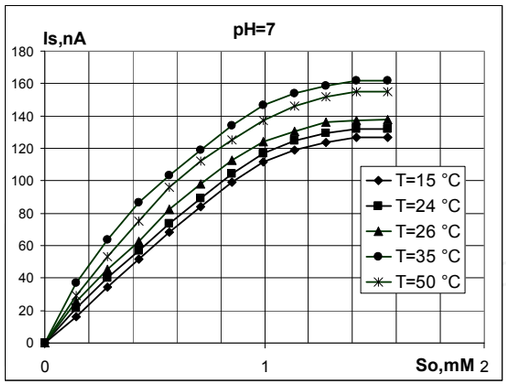

(a) Influence of temperature, pH =7

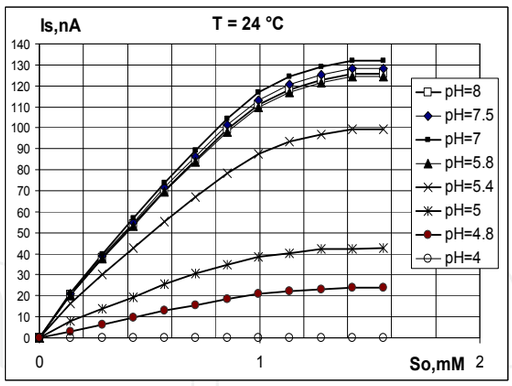

(b) Influence of pH, T = 24°C.

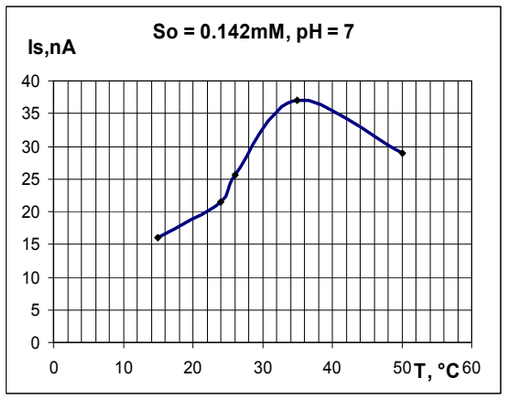

(c) Influence of temperature under constant So and pH

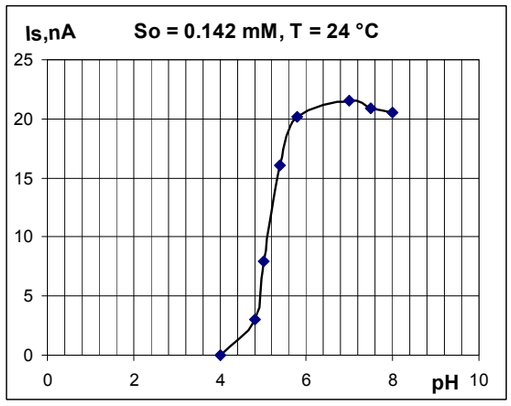

(d) Influence of pH under constant So and pH

Fig. 3. Experimental data: influences of temperature and pH on a dopamine biosensor

3. The task formulation and soft computing algorithms for its implementation

To some extent, the soft computing draws inspiration from natural phenomena. Its key areas include: neural networks, fuzzy systems, and evolutionary computation. The soft computing is usually robust under noisy input environments and has a high tolerance for imprecision in the data on which it operates. It is well known that neural networks are universal function approximators (Blum & Li, 1991). The approximation possibility of feedforward multilayered neural networks with backpropagation learning algorithm for modelling the biosensor's output voltage versus substrate concentration at different temperatures has been considered in (Ferreira et al., 2003). The same type of neural network has been used for pH estimation (Hitzman et al., 1997; Moatar et al.,1999) and control (Lamanna et al., 1996; Syu & Chen, 1998) with applications in ecology. Such neural networks have some drawbacks: (1) the proper number of hidden layers and the number of neurons in them are not known in advance, (2) the learning is a time consuming process, which often gets stuck in local minima, (3) the neural network could not generalize, if the training samples are insufficient. The CMAC-neural-network-based model of the biosensor input/output has overcome some of the drawbacks, however it needs sufficient number of

experimental data for designing a large set of overlapping receptive fields. Additional samples obtained by linear interpolation have been applied for the CMAC training in (Rangelova & Tsankova 2007a). The use of interpolated data is justified under the lack of data, because of difficulties associated with their experimental acquisition, but it reduces the main advantage of a neural model – the high accuracy. Two fuzzy logic based models of a dopamine biosensor that take into account the influence of temperature (first model) and pH (the other) have been recently proposed in (Rangelova & Tsankova, 2007b) and (Rangelova & Tsankova, 2008), respectively. This technique has been found to perform well under imprecise and insufficient experimental data.

3.1 The task formulation

The overall goal of this scientific work is to propose an appropriate soft computing technique to model the influence of both the temperature and the pH on the input-output dependency of a biosensor for dopamine assay. Due to the difficulties associated with their experimental acquisition, only very limited number of experimental data are supposed to be available. Thus, in order to accomplish the target of the work the following directions were identified:

1. To investigate and model separately the influence of temperature and pH on the output current of the above described dopamine biosensor;
2. To explore four types of soft computing techniques – CMAC, NNBP, FL and ANFIS;
3. To determine the average relative error of a few new experimental data intended for a validation of the models;
4. To select the best performing under insufficient experimental data technique;
5. To apply the selected technique for modelling the influence of both the temperature and pH (simultaneously) on the dopamine biosensor.

Since in the literature have been proposed some intelligent models, considering the influence of the temperature and the pH on the same type of biosensor, some of the here made analyses have a confirmative character (Section 5) and give us a reason to expect, that under deprived information the fuzzy model performs better than the others. That is why the fuzzy logic has been chosen *a priori* as a means for modelling simultaneously the influence of the temperature and pH. A more precise design of this model (our particular contribution here) is given in Section 4. The next two Sections (3.2 and 3.3) treat in brief some neural and fuzzy algorithms used for the purposes of intelligent modelling.

3.2 Feedforward neural networks

In this Section two types of feedforward NNs are presented: (1) CMAC-based NN, and (2) NN trained by error backpropagation learning algorithm. They are used as universal function approximators.

CMAC functional block diagram for two-dimensional input space (Miller et al., 1990) is shown in Fig. 4. A large set of overlapping, multidimensional receptive fields with finite boundaries describes the operation of the Albus CMAC (Kraft et al., 1992). Any input vector falls within the range of some of the receptive fields and excites them. The response of the CMAC neural network to a given input is the average of responses only of receptive fields excited by that input. Neural network training for a given input vector affects the adjustable parameters of the excited receptive fields. The total collection of receptive fields is divided into C subsets (layers), which represent parallel N- dimensional hyperspaces for a network with N inputs. The receptive fields in each of the layers are organized so as to span the input

space without overlapping. Any input vector excites one receptive field from each layer, which means *C* exited receptive fields per input. Each of the layers of receptive fields is offset relative to the others in the input hyperspace. The width of the receptive fields produces input generalization, while the offset of the adjacent layers of receptive fields produces input quantization (Miller & Glanz, 1994). The integer parameter *C* is determined as the *generalization parameter*. The ratio of the width of each receptive field (input generalization) to the offset between adjacent layers of receptive fields (input quantization) must be equal to *C*. Each receptive field is assumed to be a 'switch on/ switch off' type of content. If a receptive field is excited, its response is equal to the magnitude of a single adjustable weight assigned to that receptive field. If a receptive field is not excited, its response is zero. The CMAC output is the average of the adjustable weights of the excited receptive fields.

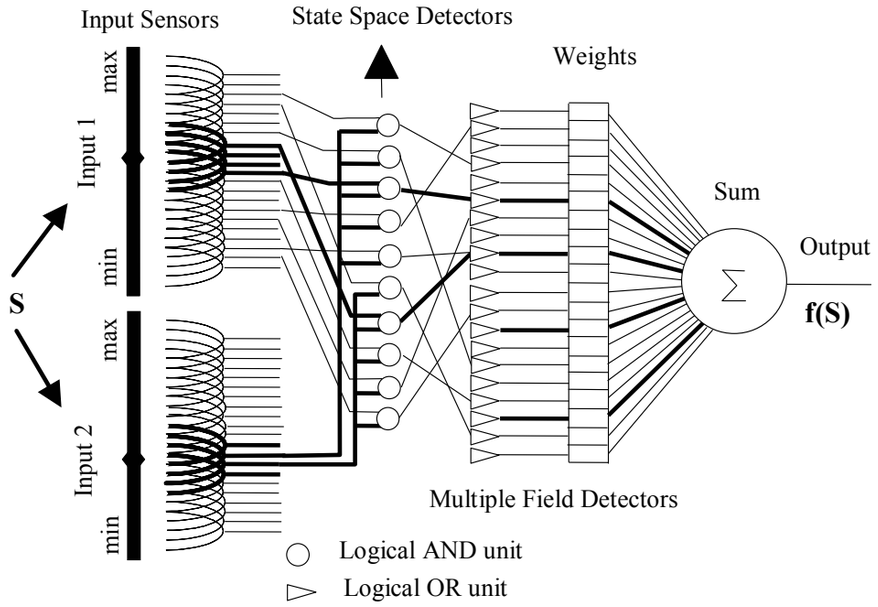

Fig. 4. CMAC functional block diagram (Kraft et al., 1992).

Consider Albus CMAC neural network with the following real valued input vector

$$\mathbf{S} = (s_1, s_2, ..., s_N)^{\mathrm{T}}, \tag{4}$$

where N is the dimension of input space. Let C be the generalization parameter (the number of simultaneously excited receptive fields for each input). The first step of the CMAC computing algorithm is to form a normalized integer input vector $\mathbf{S}'$ by dividing each component s of the input vector by an appropriate *quantization parameter* Δ_j:

$$\mathbf{S}' = (s_1', s_2', ..., s_N') = (\mathrm{int}(s_1 / \Delta_1), \mathrm{int}(s_2 / \Delta_2), ..., \mathrm{int}(s_N / \Delta_N))^T. \tag{5}$$

The width of each receptive field along the *j*th axis is equal to $C \cdot \Delta_j$ in the original input space, and is equal to C along all axes in the normalized input space. The next step of the CMAC computing algorithm is to form the vector addresses $\mathbf{A}_i$ of the C receptive fields which contain the input point $\mathbf{S}'$:

$$\mathbf{A}_i = (s'_1 - ((s'_1 - i)\%C), s'_2 - ((s'_2 - i)\%C), ..., s'_N - ((s'_N - i)\%C))^T = (a_{i1}, a_{i2}, ..., a_{iN})^T, \quad i = 1,2,...,C, \tag{6}$$

where % represents the modulus operator, and the index i references the C parallel layers of receptive fields. $\mathbf{A}_i$ is the normalized N-dimensional address of one corner of the hypercubic region spanned by the single excited receptive field in layer i. Then the next step of the CMAC algorithm is forming the scalar physical addresses A'_i of the actual adjustable weights:

$$A'_i = h(a_{i1}, a_{i2}, ..., a_{iN}). \tag{7}$$

In this equation, $h(...)$ represents any pseudo-random hashing function which operates on the components a_{ij} of the virtual addresses of the receptive fields, producing uniformly distributed scalar addresses in the physical weight memory of size M. Finally, the CMAC scalar output $y(\mathbf{S})$ is calculated as:

$$y(\mathbf{S}) = \frac{1}{C}\sum_{i=1}^{C} W(A'_i). \tag{8}$$

Network training use the data pairs $\mathbf{S}$ and $y_d(\mathbf{S})$, where $y_d(\mathbf{S})$ is the desired network output in response to the input vector $\mathbf{S}$. The weights of memory are adjusted by ΔW, calculated as:

$$\Delta W = \beta(y_d(\mathbf{S}) - y(\mathbf{S})), \tag{9}$$

where the same value ΔW is added to the content $W(A')$ of each of the C memory cells, taking part in the computation of $y(\mathbf{S})$. β is a constant training gain (between 0 and 1).
NNBP is composed of one hidden layer, whose neurons have a hyperbolic tangent sigmoid transfer function, and one neuron with a linear transfer function in the output layer. The weights of the network connections and the biases of the neuron's transfer functions are trained by the classical error backpropagation learning algorithm. Because of the limited space and the popularity of the backpropagation learning algorithm, it will not be described here. A detailed description can be found in (Rumelhart et al., 1986; Krose & Smagt, 1996).

3.3 Fuzzy logic and ANFIS

A fuzzy system employing fuzzy if-then rules can model the qualitative aspects of human knowledge and reasoning without precise quantitative analyses. Consider a fuzzy system, which comprises of four principal components: fuzzifier, fuzzy rule base, fuzzy inference engine, and defuzzifier (Fig. 5). For the sake of simplicity of understanding the mechanism of fuzzy logic the system under consideration has two inputs and one output.

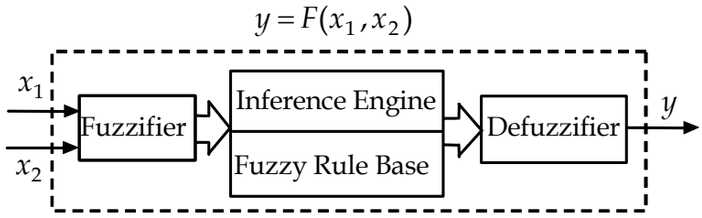

Fig. 5. Basic configuration of a fuzzy system.

Let $X_1, X_2, Y \subset R$ are universes of discourse of the variables x_1, x_2, and y, respectively. The fuzzifier performs a mapping from the observed crisp input spaces X_1 and X_2 to the fuzzy sets in these spaces. The fuzzy sets $X_1^i \in X_1$ ($i = 1,2,...,l$) and $X_2^j \in X_2$ ($j = 1,2,...,m$) are linguistic terms characterized by fuzzy membership functions $\mu_1^i(x_1)$ and $\mu_2^j(x_2)$, respectively. The two linguistic variables (for x_1 and x_2) with corresponding membership functions ($X_1^i, \mu_i(x_1)$, $X_1^{i+1}, \mu_{i+1}(x_1)$, $X_2^j, \mu_j(x_2)$, and $X_2^{j+1}, \mu_{j+1}(x_2)$) enter the fuzzy rule table. The fuzzy rule base consists of fuzzy if-then rules of Takagi and Sugeno's type (Takagi & Sugeno, 1983). The fuzzy rule set can be expressed in the following form:

$$\text{IF } x_1 \text{ is } X_1^i \text{ and } x_2 \text{ is } X_2^j \text{ THEN } y = Y_{i,j}, \tag{10}$$

where $i = 1,2,...,l$ and $j = 1,2,...,m$. Four fuzzy sets of the output signal are obtained from the fuzzy rule table: $Y_{i,j}$, $\mu_{i,j}(y)$; $Y_{i,j+1}$, $\mu_{i,j+1}(y)$; $Y_{i+1,j}$, $\mu_{i+1,j}(y)$; and $Y_{i+1,j+1}$, $\mu_{i+1,j+1}(y)$. ($Y_{i,j}$ is assumed to be the variable in the cell arranged in i-th row and j-th column of the rule table).

The *fuzzy inference engine* is a decision making logic which employs fuzzy rules from the fuzzy rule base to determine a mapping from the fuzzy sets in the input spaces X_1 and X_2 to the fuzzy sets in the output space Y. The firing strength of p,q-th rule ($\mu_{p,q}(y)$) is obtained as the T-norm of the membership values on the premise part (by using a multiplication operator):

$$\mu_{p,q}(y) = \mu_p(x_1)\mu_q(x_2), \tag{11}$$

where $p = i,\ i+1$, and $q = j,\ j+1$.

The *defuzzifier* performs a back mapping of the output signal from the fuzzy sets to crisp points. So the overall output is computed as the weighted average of each rule's output:

$$y = \frac{\sum_{p,q} Y_{p,q}\mu_{p,q}(y)}{\sum_{p,q} \mu_{p,q}(y)}, \tag{12}$$

where $p = i,\ i+1$; $q = j,\ j+1$.

ANFIS has the same number of membership functions assigned to each of the two inputs as those of the fuzzy system. A supervisor gives the training input-output samples (experimental data). The ANFIS uses a combination of least-squares and backpropagation gradient descent methods for training membership function's parameters to model that set of training data. More detailed description of ANFIS can be found in (Jang, 1993).

4. Fuzzy logic based modelling the influence of both temperature and pH on the biosensor's input/output dependency.

According to (Kosko 1992) the representation theorem states that any continuous nonlinear function can be approximated to any desired level of accuracy with a finite set of fuzzy variables, values, and rules. This theorem describes the representational power of fuzzy modelling, but it does not answer the questions, how many rules are needed and how they can be found, which are of course essential to real-world problems and solutions (Driankov

et al., 1993). In a conventional fuzzy system, the number of rules is decided by an expert who is familiar with the system to be modelled.

The experimental data needed for modelling the biosensor under consideration are given in Section 2.2 (Fig.3). The surface plot of the output current versus both pH and temperature for three different values of the substrate concentration, $S_0 = (0.142 \quad 0.426 \quad 0.710)\,\text{mM}$, is shown in Fig.6. The surfaces have the expected bell-shaped trend, forming maximum for pH=7 and temperature 35°C. Actually, only part of this experimental data, belonging to a region, that is important for the dopamine measurement, is used in the modelling process.

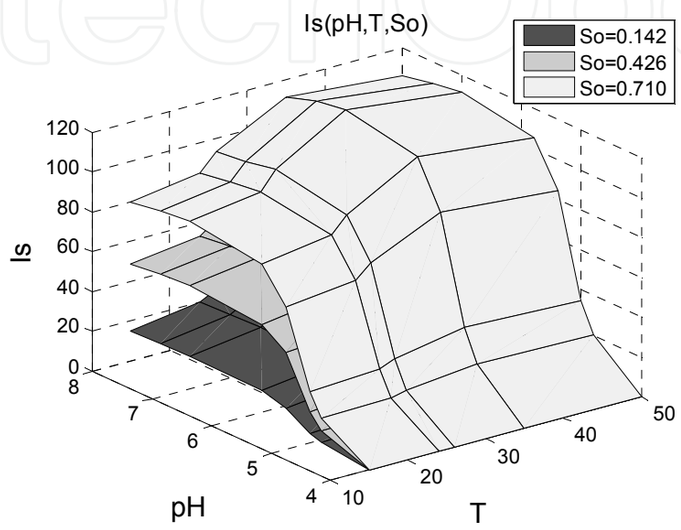

Fig. 6. Experimental data: Surface plots of the output current vs. both pH and temperature for three different values of the substrate concentration

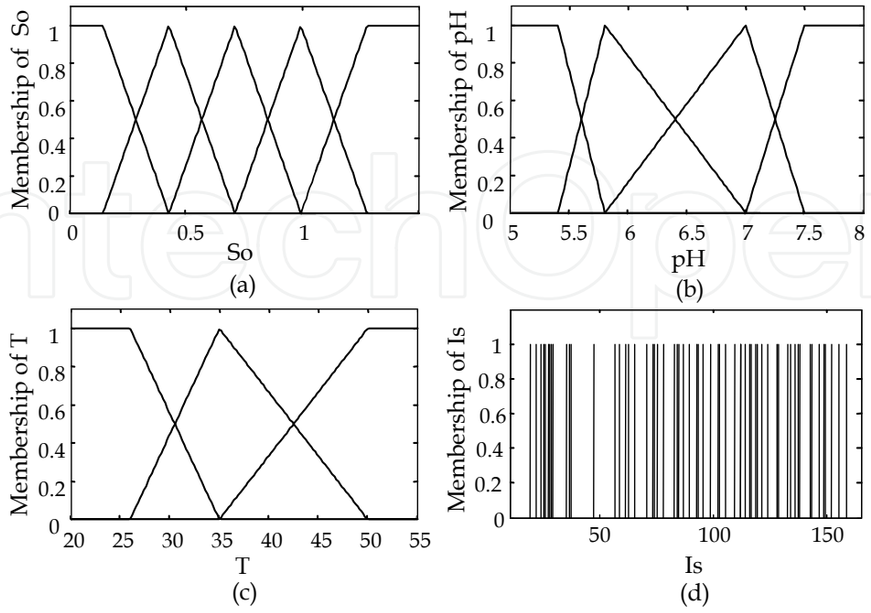

Fig. 7. Membership functions

The substrate concentration S_0, the pH and the temperature T are the three input variables of the fuzzy inference system, i.e. $x_1 \leftarrow S_0$, $x_2 \leftarrow pH$ and $x_3 \leftarrow T$. The fuzzy system described in Section 3.3 is used here, but adapted to three-dimensional input space. The number of membership functions assigned to each input variable is proposed to be equal to the number of corresponding measured values, i.e. $l = 5$ (S_0), $m = 4$ (pH) and $n = 3$ (T). In conformity with the results, reported in (Rangelova & Tsankova, 2007b; Rangelova & Tsankova, 2008) and confirmed in the next Section, the triangular shape of membership functions (Fig.7) and T-norm (using the multiplication operator) of the membership values on the premise part are chosen. The apexes of the triangles are exactly the measured values of substrate, pH and temperature. The fuzzy rule table can be filled in with all the experimental data for biosensor's output current ($y \leftarrow I_S$), which are $Y_{i,j,k} : l \times m \times n = 60$. The output current is presented by 60 different values. For the sake of convenience the values $Y_{i,j,k}$ in the fuzzy rule table are presented with 60-level gray scale squares (Fig. 8), corresponding to the values of $I_S = I_S(S_0, pH, T)$.

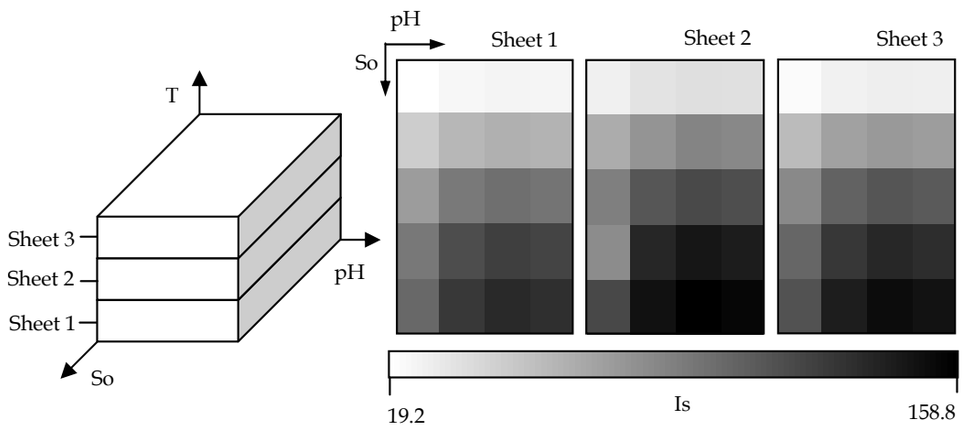

Fig. 8. Fuzzy rule table

5. Results and discussions

The next Sections 5.1 and 5.2 treat modelling the influence of the temperature and the pH separately on the biosensor's output current. The soft computing models investigated in those sections have been already proposed in the literature, and their presentation here has a confirmation character. On the basis of their comparative analysis, made in Section 5.3, the most proper type of model (sufficiently accurate under a small number of data) was chosen for the simultaneously modelling the influence of the temperature and pH on dopamine biosensor (Sections 4 and 5.4).

Fig. 9 shows the surface plots of the experimental data (Section 2.2) used in the modelling procedure of: (a) the temperature influence (pH=7), and (b) the pH influence (T=24°C).

All of the models using learning techniques need a large amount of data for training, otherwise they do not generalize incoming new data. A supervisor gives the training input-output samples. The basic samples are obtained experimentally (Fig.3, Fig9), but they are insufficient, because of difficulties associated with their experimentally deriving. This may result in a very coarse approximation or a lack of generalization. In the literature (Rangelova

& Tsankova, 2007a,b; Rangelova & Tsankova, 2008) additional samples obtained by linear interpolation have been used in training procedure.

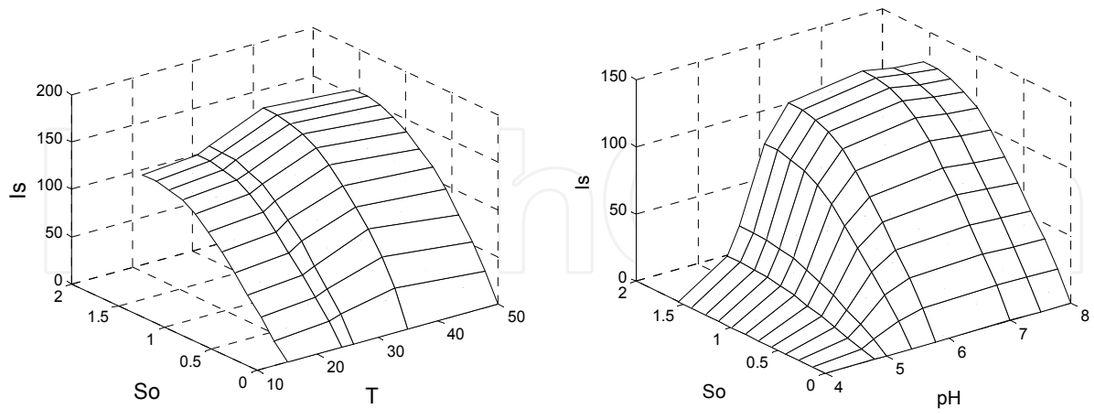

(a) (b)

Fig. 9. Surface plots of experimental data: (a) temperature influence (pH=7), and (b) *pH* influence (T=24°C)

The supervisors for both CMAC and NNBP, as well as ANFIS used the experimental data supplemented with additional samples obtained by linear interpolation with discrete parameters: (a) $0.071\,mM$ and 1^0C along substrate concentration S_0 and temperature T, respectively, in $I_S = I_S(S_0, T)$ models; and (b) $0.071\,mM$ and 0.1 along substrate concentration S_0 and pH, respectively, in $I_S = I_S(S_0, pH)$ models.
The validation of the considered aproximators is based on the average relative error over a few new experimental data (Section 5.3).

5.1 Neural networks based models of the influence of the temperature and the pH (separately) on the biosensor's output current

As it was mentioned above, in both models (the temperature influenced model and the pH influenced one), the supervisor for the CMAC neural network, as well as for the NNBP, used experimental data supplemented with additional samples.
The CMAC's generalization parameter and learning coefficient were chosen to be $C = 2$ and $\beta = 0.05$, respectively. The results obtained after 10000 learning epochs is shown in Fig.10a and Fig.10b, but after the first three thousands of iterations the accuracy of approximation was already satisfactory. The sum squared error (SSE) over the experimental data used in training (the interpolated samples are not included in the calculation of SSE) is $SSE_T^{CMAC} = 0.260$ for the temperature influenced model and $SSE_{pH}^{CMAC} = 0.423$ for the pH influenced one.
As it was mentioned in Section 3.2 the NNBP consists of one hidden layer, whose neurons posess hyperbolic tangent sigmoid transfer functions, and one output layer neuron with linear transfer function. The NNBP, modelling the temperatute influence, contained 500 neurons in its hidden layer, and the other NNBP, modelling the pH influence - 1000 neurons. After millions iterations the NNBPs were still not learned enough. The responces of the NNBP, modelling the temperatute influence and the other, modelling the pH influene (after prolonged training) are shown in Fig.10c and Fig.10d, respectively.

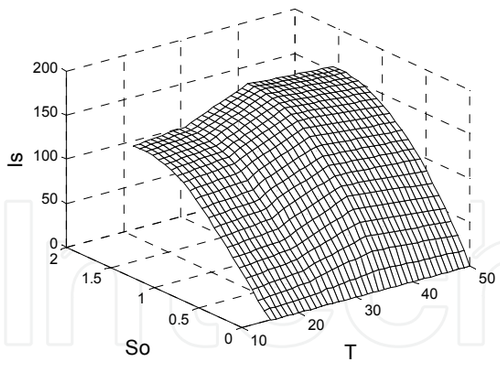

(a) CMAC model of T influence

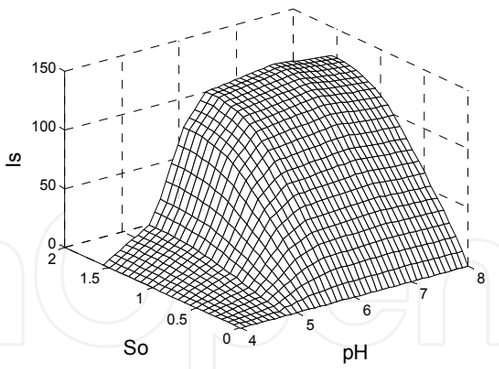

(b) CMAC model of pH influence

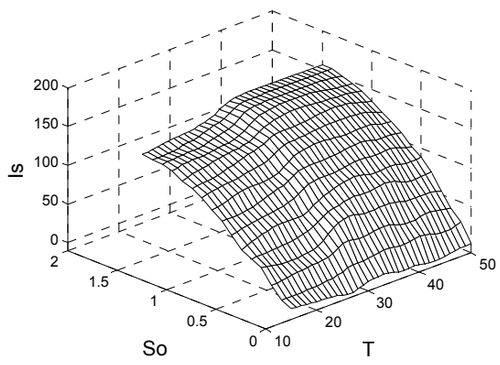

(c) NNBP model of T influence

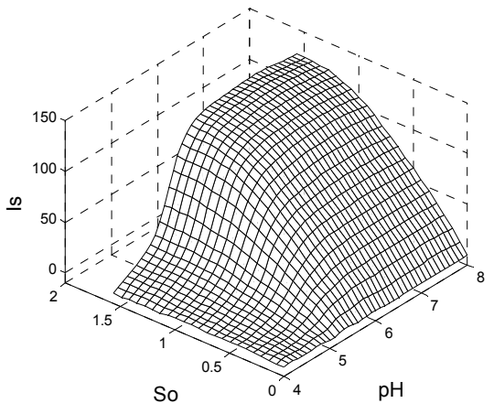

(d) NNBP model of pH influence

Fig. 10. NN-based approximation surfaces of the biosensor input/output dependency

5.2 Modelling the influence of the temperature and the pH (separately) on the biosensor's output current using fuzzy logic and ANFIS

Fuzzy logic based biosensor's model has two inputs: $x_1 \leftarrow S_0$ and $x_2 \leftarrow T$ or pH - the substrate concentration and the temperature (for the first model) or the pH (for the second model), respectively, and one output – the biosensor's current $y \leftarrow I_S$. As it was described in Section 4 the number of membership functions assigned to each input variable is equal to the number of corresponding measured values, i.e., $l = 12$ and $m = 5$ or 8 (for T or pH, respectively). The triangular form of membership functions and T-norm of the membership values on the premise part were chosen. The fuzzy rule table contained all the measurements of the biosensor's output current, which are $Y_{i,j} : l \times m = 60$ or 96 (for T or pH, respectively).

The fuzzy approximations of the biosensor's input-output relation, taking into account the influence of the temperature and the pH (separately) are shown in Fig.11a and Fig.11b, respectively. For the sake of clarity of simulations and a good visualization, discrete steps 0.071 mM, 1^0C and 0.1 pH were used along the substrate concentration, the temperature, and the pH, respectively.

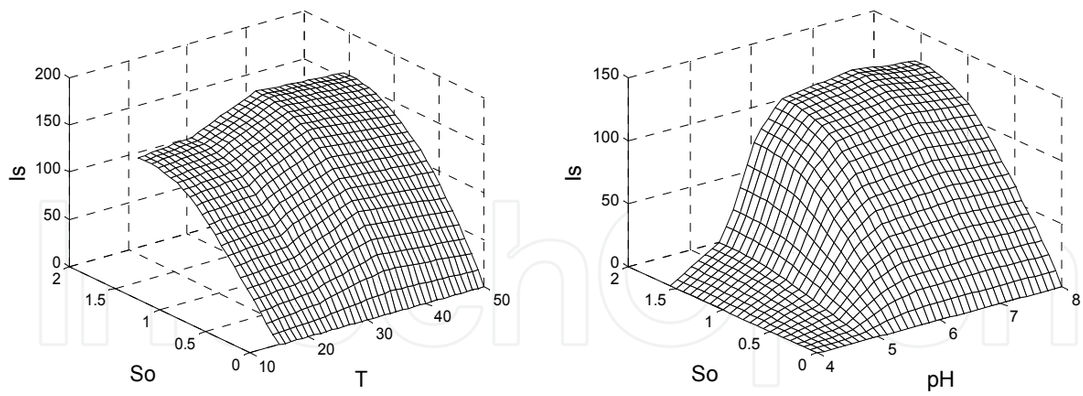

(a) (b)

Fig. 11. Fuzzy approximation surface of the influence of: (a) the temperature, and (b) the pH, on the biosensor's input-output dependency.

ANFIS had the same number of membership functions as the fuzzy approximator. Two types of membership function (MF), triangular and Gaussian curve membership functions, were heuristically chosen. The output membership function type was set up linear.

The performance of two variants of ANFIS-based approximators, one using triangular membership functions, and another - Gaussian curve based ones, is demonstrated in Fig.12a and Fig.12b, respectively. The former modelled the temperature influence on the biosensor's current, and the latter - the pH influence. In these two cases ANFIS *used only the experimental data*. Regardless of the shape of membership functions the ANFIS did not generalize under insufficient number of data. The modelling procedure was repeated with the same additional interpolated data as those used in the neural approximations. The resultant surfaces reffering to the temperatute influenced model and the pH affected one are shown in Fig.13a and Fig.13b. Both approximators shown in Fig.13 used triangular membership functions. All the ANFIS approximators were considered as trained after 20 epochs.

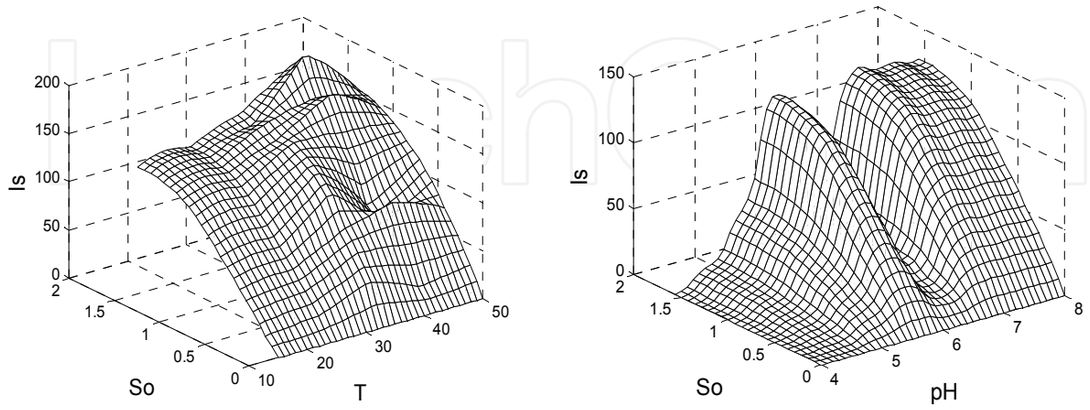

(a) ANFIS with triangular MF (model of T influence)

(b) ANFIS with Gaussian MF (model of pH influence)

Fig. 12. ANFIS-based approximation surfaces using only experimental data

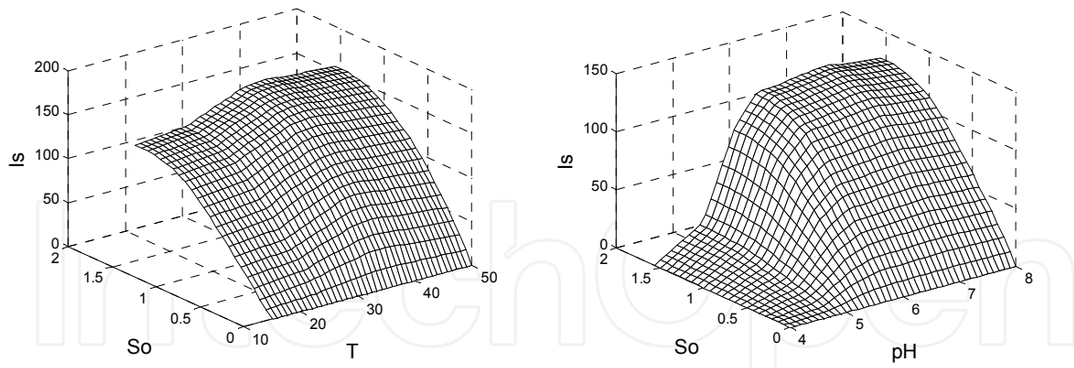

(a) ANFIS with triangular MF (model of T influence)

(b) ANFIS with triangular MF (model of pH influence)

Fig. 13. ANFIS-based approximation surfaces using additional interpolated data

5.3 Comparative analysis of the investigated models

The generalization of the four soft computing techniques was verified on the one hand qualitatively, by a visual observation the shape of approximation surfaces, and on the other hand – quantitatively, by calculating the average relative error over three new experimental samples. The relative error of each of the new experiments is calculated as

$$\varepsilon = \frac{|\, I_S^{approx} - I_S^e \,|}{I_S^e}\ 100,\ \%\qquad (13)$$

where I_S^e and I_S^{approx} are the output current determined experimentally and by means of one of the four type of approximations. The validation results, represented by the relative error (13), are listed in Table 1 and Table 2, referring to the temperature influence model and the *pH* influence one, respectively.

No.	Test Data pH = 7			NN				Fuzzy Logic		ANFIS			
				BP		CMAC				Using additional interpolated data			
										Triangular		Gaussian	
	T	S_0	I_S	I_S^{NNBP}	ε^{NNBP}	I_S^{CMAC}	ε^{CMAC}	I_S^{FL}	ε^{FL}	I_S^{ANFIS}	ε^{ANFIS}	I_S^{ANFIS}	ε^{ANFIS}
	°C	mM	nA	nA	%	nA	%	nA	%	nA	%	nA	%
1	18	0.568	70.2	72.192	2.838	70.208	0.012	70.2	0	72.80	3.706	74.60	6.271
2	18	1.136	120.8	118.782	1.671	120.902	0.085	120.9	0.083	125.96	4.272	129.84	7.483
3	25	0.710	93.3	92.601	0.750	93.698	0.427	93.7	0.429	93.67	0.396	92.99	0.332
Average Relative Error [%]					1.75		0.18		0.17		2.79		4.69

Table 1. Results from validation test for **temperature** influence modelling.

No.	Test Data T = 24°C			NN				Fuzzy Logic		ANFIS			
				BP		CMAC				Using additional interpolated data			
										Triangular		Gaussian	
	pH	S_0	I_S	I_S^{NNBP}	ε^{NNBP}	I_S^{CMAC}	ε^{CMAC}	I_S^{FL}	ε^{FL}	I_S^{ANFIS}	ε^{ANFIS}	I_S^{ANFIS}	ε^{ANFIS}
		mM	nA	nA	%	nA	%	nA	%	nA	%	nA	%
1	4.5	0.852	11.5	10.75	6.54	11.57	0.62	11.56	0.54	11.504	0.03	11.66	1.42
2	6.5	0.426	56.0	56.11	0.42	55.37	1.11	55.38	1.10	55.37	1.12	55.37	1.13
3	7.5	0.426	55.0	55.37	0.85	55.12	0.21	55.10	0.18	55.11	0.20	55.12	0.22
Average Relative Error [%]					2.60		0.65		0.61		0.45		0.92

Table 2. Results from validation test for ***pH*** influence modelling

It is evident from the two tables, that only the fuzzy approximator operates well under the small number of the experimental input/output samples. All the other approximators do not generalize under this circumstance. They need additional training data, which are obtained in this scientific work by linear interpolation of experimental data. The interpolated data predetermine the type of approximation surface and usually decrease the main advantage of neural models – the high accuracy. Using additional training data the models perform similarly to each other (with respect to accuracy), excepting the NNBP. Although the neural networks with backpropagation learning algorithm can approximate each function with sufficient high accuracy, practically, it is not so easy to determine the proper number of hidden layers and the number of neurons per each layer. Training is extremely time-consuming procedure, because it requires millions of iterations. Due to the gradient method there is a tendency the learning process to be trapped in local minima. The NNBP performs worse than the others, probably because of insufficient learning.
The fuzzy model performs better then the others: it is faster and easier to implement, works well under a small number of experimental data. These properties make it preferable for the particular purpose – to improve the accuracy of the dopamine measurement by taking into account both the temperature and the *pH* influences on the biosensor's output current.

5.4 Fuzzy modelling and validation of the simultaneous influence of temperature and pH on the biosensor's output current

The comparative analysis, made in the previous Section, shows that the most appropriate soft computing technique for our purpose (intelligent modelling the dependency $I_S = I_S(S_0, pH, T)$ using poor experimental data) is the fuzzy logic. Since this result was expected, having in mind the present publications, this model was developed and adapted to our purpose in advance in Section 4. So the membership functions of the three input variables (S_0, pH and T) and the output signal are presented in Fig.7a,b,c,d, respectively. The fuzzy rule table is shown in Fig.8. Only part of the experimental data, shown in Fig.3, is used in the fuzzy model. The samples, included in this part, correspond to the apexes of the membership functions of the input variables (Fig.7a,b,c), and more precisely written:

$$S_0 = (0.142 \quad 0.426 \quad 0.710 \quad 0.997 \quad 1.278)\ \text{mM}, \quad pH = (5.4 \quad 5.8 \quad 7.0 \quad 7.5),$$

$$\text{and} \quad T = (26 \quad 35 \quad 50)\ ^0\text{C}.$$

The fuzzy model was simulated in MATLAB environment using a number of assignment input samples and the result is shown in Fig. 14 (a qualitative validation test). For the sake of clarity two variants of a presentation (one using a gray scale, and another – colour scale) are proposed. The values of thus calculated output current I_S can be determined using the transformation bar (gray or colour bar), situated to the right of the pictures.

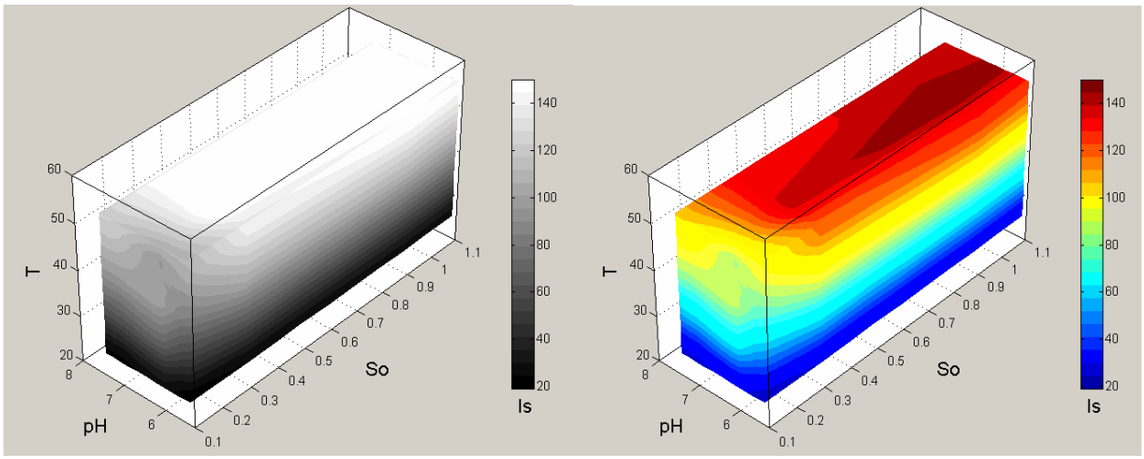

(a) (b)

Fig. 14. A plot of the biosensor's output current versus substrate concentration, temperature and pH: (a) in gray scale, and (b) in colour scale

The generalization of the fuzzy system was tested on three experimental data unused in the design process. The results are listed in Table 3 (a quantitative validation). The average relative error over the three test samples is $\bar{\varepsilon}_3^{FL} = 0.60\ \%$, and maximum relative error in this limited extract is $\varepsilon_{3,\max}^{FL} = 1.194\ \%$.

The proposed fuzzy model shows quite well results, having in mind the exceptional small extract of experimental data, needed for its design. The result inspires the idea for synthesizing a "quasi-inverse" fuzzy model in the form of $S_0 = S_0(I_S, pH, T)$, that could automate, facilitate and improve the accuracy of the dopamine measurement under variable temperature and pH.

No.	Test Data				Fuzzy Logic	
	T	pH	S_0	I_S	I_S^{FL}	ε^{FL}
	°C		mM	nA	nA	%
1	30	6.0	0.426	68.0	68.14	0.205
2	40	6.5	0.994	138.1	139.75	1.194
3	45	7.5	1.278	151.3	150.7	0.396
Average Relative Error ,%						0.60

Table 3. Results from a validation test for the simultaneous modelling the pH and T influences by means of fuzzy logic.

6. Conclusion

The presented work discusses the use of soft computing techniques for modelling the input-output dependency of a dopamine biosensor, which takes into account the simultaneous influence of pH and temperature over the output current. Under the conditions of insufficient experimental data the fuzzy approximator performs better than the others, regarding accuracy and rapidity. Besides, it does not need additional interpolated data. In order to generalize, all the other techniques, which undergo learning process, require more experimental (or interpolated) data. Moreover the learning of the NNBP is a very time consuming process and most probably could be trapped in local minima. The soft computing based modelling, as a whole, is able to improve the accuracy of a biosensor for measurement of dopamine by considering the simultaneous effect of pH and temperature on the output current. That way it provides the opportunity to have calibration surfaces for every value of the measured substrate. The algorithm can be easily programmed into a microcontroller and to be used for precise biomedical analyses. The future prospective of this work is foreseen in investigations on the simultaneous influence of the pH, temperature and dissolved oxygen concentration on the biosensor's response. The main benefit from these studies would be the possibility to expand and/or specifically adopt the resolved models over a large scale of sensing devices, sensitive to the dissolved oxygen concentration such as biosensors or microbial sensing platforms.

7. References

Blum, E. & Li, L. (1991). Approximation theory and feedforward networks, *Neural Networks*, Vol. 4, 511-515

Burket, J.; Kalil, S.; Maugeri Filho, F. & Rodrigues, M. (2006). Parameters optimization for enzymatic assays using experimental design, *Braz. J. Chem. Eng*, Vol.23, No.2, Sro Paulo Apr./June.

Castillo, J.;Gaspar, S.;Leth, S.; Niculescu, M.; Mortari, A.; Bontidean, I.; Soukharev, V.; Dorneanu, S.; Ryabov, A. & Csöregi, E. (2004). Biosensors for life quality. Design, development and applications, *Sensors and Actuators,* B 102, 179-194

Christensson, A.; Dimcheva, N.; Ferapontova, E.; Gorton, L.; Ruzgas, T.; Stoica, L.; Shleev, S.; Yaropolov, A.; Haltrich, D.; Thorneley, R. & Aust, S. (2004). Direct electron transfer between ligninolytic redox enzymes and electrodes, *Electroanalysis*, Vol.16, No.13-14, 1074-1092 (a review)

Climent, P.; Serralheiro, M. & Rebelo, M. (2001). Development of a new amperometric biosensor based on polyphenoloxidase and polyethersulphone membrane, *Pure Appl. Chem.*, Vol. 73, No. 12, 1993–1999

David, F.(1997). Amperometric Oxygen Electrodes, *Bioanalytical Systems, Inc.,* Vol. 16 No. 1

Dimcheva, N.; Horozova E. & Jordanova, Z. (2002). A Glucose Oxidase Immobilized Electrode Based on Modified Graphite. *Zeitschrift fur Naturforschung,* No. 57C, 705-711

Dodevska, T.; Horozova, E. & Dimcheva, N. (2006). Electrocatalytic reduction of hydrogen peroxide on modified graphite electrodes: application to the development of glucose biosensors. *Anal. Bioanal. Chem.*, Vol., 386, No.5, 1413-1418

Driankov, D.; Hellendoorn, H. & Reinfrank, M. (1993). *An Introduction to Fuzzy Control*, Springer-Verlag Berlin Heidelberg, USA

Ferreira, L.; Souza Jr, M.; Trierweiler, J.; Hitzmann, B & Folly, R.(2003). Analysis of experimental biosensor/FIA lactose measurements, *Brazilian Journal of Chemical Engineering*, Vol. 20, No. 1

Hitzmann, B. et al.(1997). Computational neural networks for the evaluation of biosensor FIA measurements, *Analytica Chimica Acta,* Vol.348, 135-141

Horozova, E.; Dodevska, T. & Dimcheva, N. (2009). Modified graphites: Application to the development of enzyme-based amperometric biosensors, *Bioelectrochemistry* , No.74 260 - 264

Jang, J.(1993). ANFIS: Adaptive-network-based fuzzy inference system, *IEEE Trans. on Systems, Man and Cybernetics*, Vol. 23, No. 3, pp. 665-685, May

Kosko, B. (1992). *Neural Networks and Fuzzy Systems. A Dynamical Systems Approach to Machine Intelligence*, Prentice-Hall Inc

Kraft, L, , Miller, W. & Dietz, D. (1992). *Development and application of CMAC neural network-based control*, Handbook of Intelligent Control. Neural, Fuzzy, and Adaptive Approaches. D.A. White, D.A. Sofge (Eds.), Multiscience Press, Inc., USA, 215-232

Krose, B. & Van der Smagt, P. (1996). *An Introduction to Neural Networks*, 8th ed., The University of Amsterdam, September 1996

Lamanna, R.; Uria, M.; Kelly, J. & Pinto, E.(1996). Neural network based control of pH in a laboratory-scale plant, International Workshop on Neural Networks for Identification, Control*, Robotics, and Signal/Image Processing (NICROSP '96)*, pp.314-320

Moatar, F., Fessant, F. & Poirel, A. (1999) . pH modelling by neural networks. Application of control and validation data series in the Middle Loire river, *Ecological Modelling*, Vol. 120, No.2-3, 141-156

Miller, W., Glanz, F. & Kraft, L. (1990). CMAC an associative neural network alternative to backpropagation, *IEEE Proceedings* 78, 1561-1567

Miller, W. & Glanz, F.(1994). UNH_CMAC Version 2.1: The University of New Hampshire implementation of the Cerebellar model arithmetic computer - CMAC, http://www.ece.unh.edu/robots/ unh_cmac.ps

Palmer, J. Banana polyphenoloxidase. Preparation and Properties (1963) Preparation and properties, *Plant Physiology*, No.38, 508-513

Patent Application (2006) U.S. Provisional No. 60/859,586, filed Nov. 16, 2006, entitled "Temperature compensation for enzyme electrodes "

Puida, M.; Ivanauskas, F. & Laurinavicius, V. (2009), Mathematical modeling of the action of biosensor possessing variable parameters, *J Math Chem,* DOI 10.1007/s10910-009-9541-5, Springer Science+Business Media, LLC 2009

Rangelova, V., Kodjabashev,I. & Al. Neykov. (2002) Investigation of Repeatability and Error Instability Analysis of Tissue Biosensor, *Proceedings. of II Int. Symp. "Instrumentation Science and Technology- Isist2002"*, 18-22 aug 2002, Jinan City, China, vol.3, pp.231-238

Rangelova, V. (2003). Investigation of influence of thickness of active membrane of constructed tissue biosensor. *Journal of TU-Plovdiv, Fundamental Sciences and Applications*, Vol.10, 23-28, Bulgaria

Rangelova, V. & Tsankova, D. (2007a). CMAC-based modelling the influence of temperature on tissue biosensor for measurement of dopamine, *Proc. of the 5th IASTED International Conference Biomedical Engineering (BioMED 2007)*, Innsbruck, Austria, pp.15-19.

Rangelova, V. & Tsankova, D. (2007b). Fuzzy-based modelling the influence of temperature on tissue biosensor for measurement of dopamine, *Proc. of the 15th Mediterranean Conference on Control and Automation – MED'07*, Athens, Greece, 27-29 June, 2007, Paper No. T12-008

Rangelova, V. & Tsankova, D. (2008). Soft computing techniques in modeling the influence of pH on dopamine biosensor, *Proc. of the 4th International IEEE Conference on Intelligent systems – IS'08*, Varna, Bulgaria, pp. 12-23

Rumelhart, D.E.; Hinton, G.E., & Williams, R.J. (1986). Learning internal representations by error propagation. In: *Parallel Data Processing*, Rumelhart, D.E. & McClelland, J., (Eds.), Vol.1, Ch. 8, pp. 318-362, Cambridge, MA: M.I.T. Press

Scheller, F.; Wollenberger, U.; Warsinke, A. & Lisdat, F. (2001). Research and development in biosensors, *Current Opinion in Biotechnology,* No 12, 35–40

Shizuko, H. et al., (2005). Biosensor Based on Xanthine Oxidase for Monitoring Hypo-xanthine in Fish Meat, *American Journal of Biochemistry and Biotechnology,* Vol.1, No.2, 85-89

Syu, M.&Chen, B. (1998). Back-propagation neural network adaptive control of a continuous wastewater treatment process, *Ind. Eng. Chem. Res.,* Vol. 37, No. 9, pp. 3625 -3630

Skladal, P. (1995). Compensation of temperature variations disturbing performance of an amperometric biosensor for continuous monitoring. *Sensors and actuators. B, Chemical* , Vol. 28, No1, pp. 59-62

Stoica, L.; Dimcheva, N.; Haltrich, D.; Ruzgas, T. & Gorton, L.(2005). Electrochemical investigation of direct electron transfer between cellobiose dehydrogenase from new fungal sources on Au electrodes modified with different alkanethiols. *Biosensors and Bioelectronic,s* , No20, 2010–2018

Stoica, L., Dimcheva, N.; Ackermann, Y.; Karnicka, K.; Guschin, D.; Kulesza, P.; Rogalski, J.; Haltrich, D.; Ludwig, R.; Gorton, L. & Schuhmann, W. (2009). Membrane-less biofuel cell based on cellobiose dehydrogenase (anode)/laccase (cathode) wired via specific Os-redox polymers, *Fuel Cells* ,No.9, 53-62

Takagi, T. & Sugeno, M. (1983). Derivation of fuzzy control rules from human operator's control actions, *Proceedings. of the IFAC Symp. on Fuzzy Information, Knowledge Representation and Decision Analysis*, pp. 55–60, July

Ziyan, E. & Pekyardimci, S. (2004). Purifcation and Characterization of Pear Polyphenol Oxidase, *Turk J Chem*, No.28 , 547 - 557

Used denotations

ANFIS - Adaptive-network-based fuzzy inference system
BOD - Biological oxygen demand

CMAC - Cerebellar Model Articulation Controller
FL - Fuzzy logic
MF - Membership function
NNBP - Neural network with backpropagation learning algorithm
PPO - Polyphenol oxidase
SSE - Sum squared error

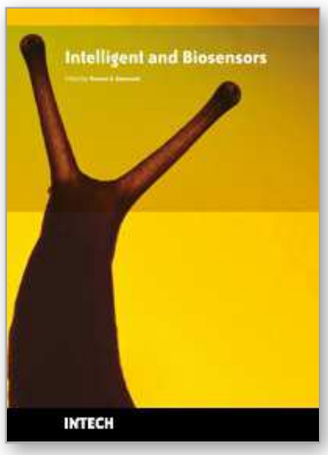

Intelligent and Biosensors

Edited by Vernon S. Somerset

ISBN 978-953-7619-58-9
Hard cover, 386 pages
Publisher InTech
Published online 01, January, 2010
Published in print edition January, 2010

The use of intelligent sensors have revolutionized the way in which we gather data from the world around us, how we extract useful information from that data, and the manner in which we use the newly obtained information for various operations and decision making. This book is an attempt to highlight the current research in the field of Intelligent and Biosensors, thereby describing state-of-the-art techniques in the field and emerging new technologies, also showcasing some examples and applications.

InTech Europe
University Campus STeP Ri
Slavka Krautzeka 83/A
51000 Rijeka, Croatia
Phone: +385 (51) 770 447
Fax: +385 (51) 686 166
www.intechopen.com

InTech China
Unit 405, Office Block, Hotel Equatorial Shanghai
No.65, Yan An Road (West), Shanghai, 200040, China
中国上海市延安西路65号上海国际贵都大饭店办公楼405单元
Phone: +86-21-62489820
Fax: +86-21-62489821

IntechOpen